

Soft Tissue Engineering, PhD Thesis,
Mechanical and *In Vitro* Performance of
Foam Replication Technique, *Acta*
Five Glass Scaffolds for Bone Tissue
Selective Laser Sintering Fabrication
Materials Science & Technology Annual
Strong Glass Scaffolds, *Adv. Funct.*
In Vivo Evaluation of 13-93 Bioactive
in a Subcutaneous Rat Implantation

DO CELL CULTURE SOLUTIONS TRANSFORM BRUSHITE ($\text{CaHPO}_4 \cdot 2\text{H}_2\text{O}$) TO OCTACALCIUM PHOSPHATE ($\text{Ca}_8(\text{HPO}_4)_2(\text{PO}_4)_4 \cdot 5\text{H}_2\text{O}$)?

Ibrahim Mert, Selen Mandel, and A. Cuneyt Tas
Department of Biomedical Engineering, Yeditepe University, Istanbul 34755, Turkey

ABSTRACT

The purpose of this study was to investigate the transformation of brushite (dicalcium phosphate dihydrate, DCPD, $\text{CaHPO}_4 \cdot 2\text{H}_2\text{O}$) powders at 36.5 C in DMEM (Dulbecco's Modified Eagle Medium) solutions. Two sets of brushite powders with different particle shapes were synthesized to use in the above DMEM study. The first of these brushite powders was prepared by using a method which consisted of stirring calcite (CaCO_3) powders in a solution of ammonium dihydrogen phosphate ($\text{NH}_4\text{H}_2\text{PO}_4$) from 6 to 60 minutes at room temperature. These powders were found to consist of dumbbells of water lily-shaped crystals. The second one of the brushite powders had the common flat plate morphology. Both powders were separately tested in DMEM-immersion experiments. Monetite (DCPA , CaHPO_4) powders were synthesized with a unique water lily morphology by heating the water lily-shaped brushite crystals at 200 C for 2h. Brushite powders were found to transform into octacalcium phosphate (OCP, $\text{Ca}_8(\text{HPO}_4)_2(\text{PO}_4)_4 \cdot 5\text{H}_2\text{O}$) upon soaking in DMEM (Dulbecco's Modified Eagle Medium) solutions at 36.5 C over a period of 1 day to 1 week. Brushite powders were known to transform into apatite when immersed in synthetic (simulated) body fluid (SBF) solutions. This study found that DMEM solutions are able to convert brushite into OCP, instead of apatite.

INTRODUCTION

DMEM (Dulbecco's Modified Eagle Medium) solutions are used in cell culture as the growth medium. HEPES-buffered DMEM solutions contain inorganic salts (to supply Ca^{2+} , Mg^{2+} , Na^+ , K^+ , Fe^{3+} , H_2PO_4^- , HCO_3^- and Cl^- ions), amino acids, vitamins and glucose. DMEM solutions have a Ca/P molar ratio of 1.99.

SBF (simulated [1] or synthetic body fluid [2]) solutions, on the other hand, are usually TRIS- or HEPES-buffered [3] and only contain inorganic salts with an overall Ca/P molar ratio of 2.50.

DMEM solutions are one of the best media to test the bioactivity of synthetic biomaterials. Bioactivity of any material cannot be tested in SBF solutions. SBF solutions cannot be used in cell culture studies since they lack the necessary nutrients, such as amino acids, vitamins and glucose, to allow and sustain the proliferation of living organisms.

However, SBF solutions were heavily used in recent decades to test the so-called and deceptive bioactivity of a given material, regardless of being metallic, ceramic, glassy or polymeric. Can bioactivity be tested *in vitro* with SBF solution [4]? How useful is SBF in predicting *in vivo* bone bioactivity [5]? These two questions were previously asked and had actually become the exact titles of two articles cited here [4, 5]. SBF solutions are metastable and supersaturated solutions (they are supersaturated with respect to the formation of apatite-like, i.e., apatitic, calcium phosphate (CaP) phase) and SBF solutions would thus automatically precipitate apatitic CaP on substances with basic surfaces immersed in them. Precipitation of an apatite-like phase and bioactivity were simply two diverse concepts which were often confused in the literature very seriously [4, 5].

Nevertheless, the following question has not been asked frequently; could it be possible to test, *in vitro*, such a so-called bioactivity by using readily available DMEM solutions, containing amino acids, vitamins and glucose, instead of SBFs? The current study asks this question in search of an answer to it, by ageing brushite (dicalcium phosphate dihydrate, DCPD, $\text{CaHPO}_4 \cdot 2\text{H}_2\text{O}$) powders in DMEM solutions at 36.5 C.

Two different, chemically-synthesized $\text{CaHPO}_4 \cdot 2\text{H}_2\text{O}$ powders with quite different particle morphologies were tested by soaking them in DMEM solutions at the human body temperature of 36.5 °C from 1 day to 1 week.

Brushite is a relatively high solubility (with $\log K_{\text{sp}}$ of -6.6 [6]) calcium phosphate compound and is known to convert into apatite-like calcium phosphate when soaked in SBF solutions at the human body temperature for about one week [7-21].

However, both of the brushite powders used in this study [22] were found to transform into octacalcium phosphate (OCP, $\text{Ca}_8(\text{HPO}_4)_2(\text{PO}_4)_4 \cdot 5\text{H}_2\text{O}$) when soaked in DMEM solutions. To the best of our knowledge, this study was the first to report on the bulk transformation of brushite powders into OCP upon soaking in a common cell culture solution, such as DMEM.

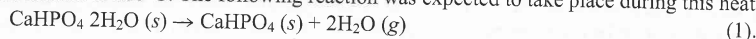
EXPERIMENTAL PROCEDURE

Synthesis of Brushite or Monetite with Water Lily-shaped (WL) Crystals

Brushite (DCPD, $\text{CaHPO}_4 \cdot 2\text{H}_2\text{O}$) powders with a unique water lily- morphology were synthesized as follows. 40.0 g (=0.3477 mol P) of ammonium dihydrogen phosphate, $\text{NH}_4\text{H}_2\text{PO}_4$ ($\geq 99.9\%$, Cat. No: 1.01126, Merck KGaA, Darmstadt, Germany) was first dissolved in 340 mL of distilled water. This solution had a pH value of 3.9 ± 0.1 at room temperature (RT). The solution was placed into a 500 mL-capacity Pyrex glass media bottle. 10.0 g (=0.0999 mol Ca) of calcite (precipitated-chalk type), CaCO_3 ($\geq 99.9\%$, Cat. No: 12010, Riedel-de-Haen, Germany) powder was added into the bottle. The formed suspension was stirred (500 rpm) at RT for 30 minutes, by using a Teflon-coated magnetic stirrer. After 30 min of stirring, the pH value of the white suspension was measured to be 5.9 ± 0.1 . The particles of the suspension were recovered from their mother liquor by using a porcelain Buechner funnel containing a No. 3 Whatman filter paper. The funnel was attached to a mechanical vacuum pump during filtration. The wet cake on the filter paper was finally washed with 750 mL of distilled water. Obtained powders were dried in a clean watch-glass overnight at 75 °C, in a static air microprocessor-controlled oven, to obtain 14.64 ± 0.2 g of brushite with the water lily (WL, *Nymphaeaceae*) morphology. After the addition of precipitated-chalk type CaCO_3 powder into the above-mentioned $\text{NH}_4\text{H}_2\text{PO}_4$ solution, stirring was not a necessity; the same results would have been obtained if one were to choose to keep the resultant white suspension "non-stirred" for an overnight period (typically 18 to 19 hours).

The above was the optimized and up-scaled synthesis recipe of the WL-shaped brushite powders. Prior to the development of this recipe, the influence of stirring time on the advance of reaction was studied over the range of 90 seconds to 60 minutes. In these experiments, 10.0 g of $\text{NH}_4\text{H}_2\text{PO}_4$ was first dissolved in 85 mL of distilled water and then stirred at RT with 2.5 g of calcite (CaCO_3) powder in 100 mL-capacity glass bottles containing 85 mL distilled water.

To convert the WL-shaped brushite crystals into monetite (DCPA, CaHPO_4), 1.0 g of the above brushite powders was kept (in clean watch glasses) for 2 hours in a microprocessor-controlled static air oven pre-heated to 200 °C. The following reaction was expected to take place during this heating;



Synthesis of Brushite with Flat Plate-shaped (FP) Crystals

The synthesis procedure used to form flat plate-shaped brushite crystals simply consisted of preparing two solutions. Solution A was prepared as follows: 0.825 g of KH_2PO_4 ($\geq 99.9\%$, Cat. No: 1.04873, Merck KGaA) was dissolved in 700 mL of distilled water, followed by the addition of 3.013 g of Na_2HPO_4 ($\geq 99.9\%$, Cat. No: 1.06586, Merck KGaA), which resulted in a clear solution of pH 7.5 at RT. Solution B (of pH 6.4) was prepared by dissolving 4.014 g of $\text{CaCl}_2 \cdot 2\text{H}_2\text{O}$ ($\geq 99.9\%$, Cat. No: 1.02382, Merck KGaA) 200 mL of distilled water. Solution B was then rapidly added to solution A and the precipitates formed were aged for 80 min at RT, by continuous stirring at 500 rpm (final

solution pH 5.3). Solids recovered by filtration were washed with distilled water to obtain 3.28 g of FP-shaped brushite.

Transformation of WL-shaped Brushite

Glass media bottles (100 mL-capacity, glucose 1X, Sterile, Product No: 21063-100, Corning) were used for the study. The DMEM solutions of this study were placed in each bottle and the plastic caps were placed in a microprocessor-controlled static air oven for ageing the brushite powders in DMEM solution of the one week sample. At the end of the specified ageing periods, the solution was filtered through a Whatman No. 1 Buechner funnel and No. 2 Whatman filter paper. The solids were washed with 500 mL of distilled water. Washed solids were dried in a clean watch-glass overnight. DMEM-transformed powders with the WL morphology were aged for 24 h, 48 h and one week-aged samples.

Transformation of FL-shaped Brushite

Glass media bottles (100 mL-capacity, glucose 1X, Sterile, Product No: 21063-100, Corning) were used for the study. The brushite powder was placed in each bottle and the plastic caps were placed in a microprocessor-controlled static air oven for ageing the brushite powders in DMEM solution of the one week sample. At the end of the specified ageing periods, the solution was filtered through a Whatman No. 1 Buechner funnel and No. 2 Whatman filter paper. The solids were washed with 500 mL of distilled water. Washed solids were dried in a clean watch-glass overnight. FL-transformed powders with the FL morphology were aged for 24 h, 48 h and one week-aged samples.

Sample Characterization

All powder samples were characterized by X-ray diffraction (XRD) using a Bruker AG, Karlsruhe, Germany) after the samples were dried in a vacuum oven. Samples were scanned with a step size of 0.02 ° (EVO 40, Zeiss, Dresden, Germany) was used. The samples were sputter-coated, prior to impedance spectroscopy to improve conductivity to the specimen surfaces. For scanning electron microscopy (SEM) analyses were performed using a JEOL JSM-6300LV powder, followed by compacting those samples into pellets. FTIR data were recorded over the range of 4000-400 cm^{-1} .

RESULTS

The X-ray diffraction (XRD) and FTIR analyses of brushite powders (denoted as FP and WL) are shown in Fig. 1a and 1b. The XRD spectra given in Fig. 1b depicted that the brushite powders of mixing was not enough and the calcite phase was observed. The stirring as short as 6 minutes brushite was

solution pH 5.3). Solids recovered by filtration from their mother liquors were dried overnight at 65°C to obtain 3.28 g of FP-shaped brushite powders.

Transformation of WL-shaped Brushite into OCP in DMEM Solution

Glass media bottles (100 mL-capacity) containing 50 mL of DMEM solutions (DMEM, High glucose 1X, Sterile, Product No: 21063-029, Gibco, Invitrogen, USA) were used. The composition of the DMEM solutions of this study were given elsewhere [22]. 1.0 g of WL-shaped brushite powder was placed in each bottle and the plastic caps of the bottles were sealed. The bottles were placed in a microprocessor-controlled static air oven whose temperature was adjusted to 36.5±0.1°C. The times for ageing the brushite powders in DMEM solutions were selected as 24, 48 h and one week. The DMEM solution of the one week sample was replenished with a fresh solution after 120 h. At the end of the specified ageing periods, the solids were recovered from the solutions by using a porcelain Buechner funnel and No. 2 Whatman filter paper, with vacuum filtration. The solids were washed with 500 mL of distilled water. Washed samples were left to dry overnight at 65°C to finally obtain DMEM-transformed powders with the following weights; 0.80±0.03 g, 0.81±0.03 g, 0.70±0.03 g for the 24 h-, 48 h- and one week-aged samples, respectively.

Transformation of FL-shaped Brushite into OCP in DMEM Solution

Glass media bottles (100 mL-capacity) containing 50 mL of DMEM solutions (DMEM, High glucose 1X, Sterile, Product No: 21063-029, Gibco, Invitrogen, USA) were used. 0.65 g of FP-shaped brushite powder was placed in each bottle and the plastic caps of the bottles were sealed. The bottles were placed in a microprocessor-controlled static air oven whose temperature was adjusted to 36.5±0.1°C. The times for ageing the FL-type brushite powders in DMEM solutions were selected as 48 h and one week. The DMEM solution of the one week sample was replenished with a fresh solution at every 48 hours. At the end of the specified ageing periods, the solids were recovered from the solutions by using a porcelain Buechner funnel and No. 2 Whatman filter paper, with vacuum filtration. The solids were washed with 500 mL of distilled water. Washed samples were left to dry overnight at 65°C to finally obtain DMEM-transformed powders with the following weights; 0.46±0.01 g and 0.45±0.01 g for the 48 h- and one week-aged samples, respectively.

Sample Characterization

All powder samples were characterized by using a powder X-ray diffractometer (Advance D8, Bruker AG, Karlsruhe, Germany) after being lightly grinded by an agate mortar and pestle. The diffractometer was operated with a Cu tube at 40 kV and 40 mA equipped with a monochromator. Samples were scanned with a step size of 0.02° and a preset time of 5 s. Scanning electron microscopy (EVO 40, Zeiss, Dresden, Germany) was used to evaluate the morphology of the powder samples. The samples were sputter-coated, prior to imaging, with a 25 nm-thick gold layer to impart electrical conductivity to the specimen surfaces. Fourier-transform infrared spectroscopy (Spectrum One, Perkin Elmer, USA) analyses were performed after mixing 1 mg of sample powders with 300 mg of KBr powder, followed by compacting those into a thin pellet in a stainless steel die of 1 cm inner diameter. FTIR data were recorded over the range of 4000 to 400 cm⁻¹ with 128 scans.

RESULTS

The X-ray diffraction (XRD) and Fourier-transform infrared (FTIR) spectra of the two different brushite powders (denoted as FP and WL powders) synthesized in this study are given in Fig. 1a. The XRD spectra given in Fig. 1b depicted that the for the synthesis of WL-shaped brushite crystals, 90 s of mixing was not enough and the calcite powders remained still unreacted after 90 s, but in a time of stirring as short as 6 minutes brushite was forming in the aqueous CaCO₃-NH₄H₂PO₄ suspensions.

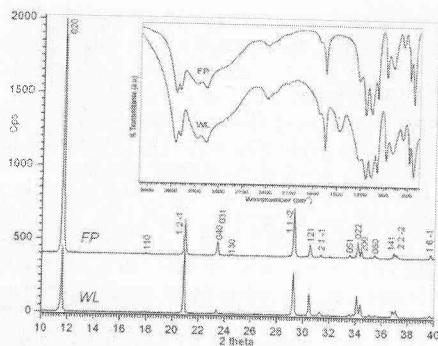


Fig. 1a XRD spectra of WL- (30 min stirring) and FP-type brushite powders; inset is depicting the FTIR spectrum of WL (30 min) and FP-type brushite

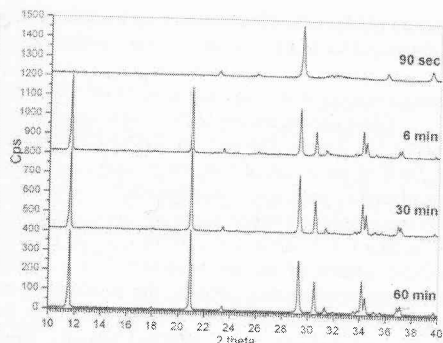


Fig. 1b XRD spectra of WL samples as a function of stirring time; 90 s trace was single-phase calcite, the other were pure brushite

Therefore, the selection of a mixing time between 6 and 60 minutes would be appropriate. There were no changes in the crystal size and shape of WL-type brushite powders if one increased the mixing time from 6 to 30 min or from 30 to 60 minutes. The scanning electron photomicrograph (SEM) of WL-type powders was shown in Fig. 1c.

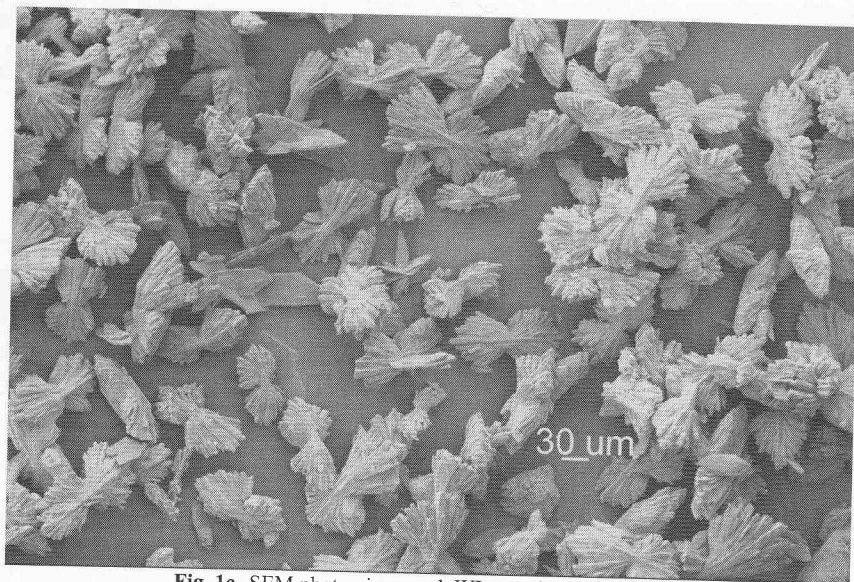


Fig. 1c SEM photomicrograph WL-type brushite crystals

FP (flat-plate) powders consisted of large and flat plates of brushite, with a preferred growth along the (020) crystallographic planes and the relatively high X-ray intensities obtained from these

planes were apparent in the top XRD trace (150 nm), had a width between 5 to 10 μm. This morphology is quite common to the precipitates in the literature on brushite. On the other hand, the morphology of this study comprised dumbbells of water molecules 80-100 μm in size. For the WL-type brushite, the X-ray intensities for the (020) and (1 2 -1) reflections were not reported prior to this study [22].

The FTIR inset shown in Fig. 1a displays the presence of unreacted CaCO₃, which was not detected in the XRD trace. The SEM morphology of the CaCO₃ powders used in this study for the synthesis of WL-type brushite, these CaCO₃ particles were behaving as the template and a new phase was formed in place of the original template. Such a phase could be regarded as reasonable to have unreacted CaCO₃ at their cores. Such WL-type brushite was not reported prior to this study [22].

The XRD, FTIR and SEM data given in this study were obtained from the 200 C-heating (for 2 h) of the brushite. The brushite-to-monite transformation preserved the WL morphology. Brushite-to-monite transformation involves the loss of two water molecules. Our 200 C-heating of the brushite powders with this WL-type particle morphology was reported before. Commercially available monite powder (whose SEM morphology was reported

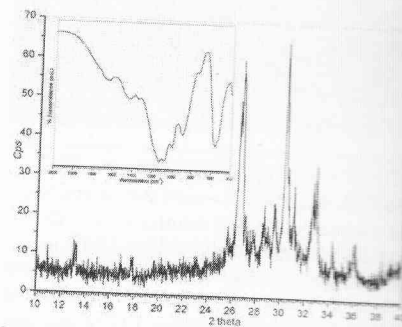


Fig. 2a XRD and FTIR (inset) spectra of monite (CaHPO₄) powders of WL type

Brushite crystallizes in the monoclinic system with $a=11.85$ Å, $b=15.177$ Å, $c=5.81$ Å, $\beta=118.54^\circ$ [25]. Triclinic brushite has $a=11.85$ Å, $b=6.627$ Å, $c=6.998$ Å, $\alpha=96.34^\circ$, $\beta=103.82^\circ$, and $\gamma=103.82^\circ$.

planes were apparent in the top XRD trace of Fig. 1a. Those flat-plates were found to be thin (about 150 nm), had a width between 5 to 10 μm , and could elongate to about 70 to 80 μm . Flat-plate morphology is quite common to the precipitated brushite powders and could be frequently encountered in the literature on brushite. On the other hand, the WL (water lily, *Nymphaeaceae*) brushite powders of this study comprised dumbbells of water lily-shaped crystals. These crystals were again large, about 80-100 μm in size. For the WL-type brushite crystals (in comparison to the FP powders) almost equal X-ray intensities for the (020) and (1 2 -1) planes were registered as seen in Fig. 1a; i.e., the bottom XRD trace.

The FTIR inset shown in Fig. 1a disclosed that the WL powders contained a certain amount of unreacted CaCO_3 , which was not detected by the XRD spectra of the same powders. The starting powder for the WL-type brushite was precipitated-chalk type CaCO_3 spindle-shaped particles. The SEM morphology of the CaCO_3 powders used in the current study was given elsewhere [23]. During the synthesis of WL-type brushite, these CaCO_3 (calcite) particles were chemically attacked by the acidic H_2PO_4^- ions in solution, and a templated synthesis-type reaction followed that. The calcite particles were behaving as the template and the dumbbells of stacked brushite water lilies gradually formed in place of the original template. Since this was a room temperature aqueous reaction starting from the surface of the calcite template particles and advancing with time toward the cores of particles, it could be regarded as reasonable to have very small amounts (i.e., not detectable by the X-rays) of unreacted CaCO_3 at their cores. Such WL-shaped brushite crystals, to the best of our knowledge, were not reported prior to this study [22].

The XRD, FTIR and SEM data given in Fig. 2 denoted that the monetite (CaHPO_4) powders obtained from the 200 C-heating (for 2 h) of WL-brushite powders were single-phase and still preserved the WL morphology. Brushite-to-monetite conversion follows a simple dehydration reaction. The theoretical weight loss in the brushite-to-monetite conversion is 20.94%, which represents the loss of two water molecules. Our 200 C-heating runs always exhibited around 21% weight loss. Monetite powders with this WL-type particle morphology, to the best of our knowledge, were again not reported before. Commercially available monetite powders typically comprise rectangular prismatic or cubic particles (whose SEM morphology was reported elsewhere [24]).

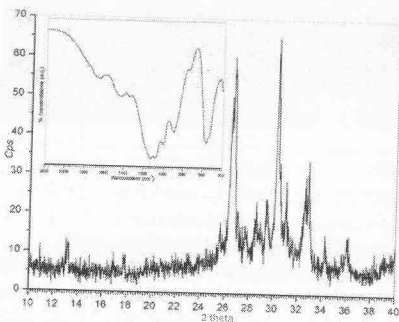


Fig. 2a XRD and FTIR (inset) spectra of monetite (CaHPO_4) powders of WL type



Fig. 2b Characteristic SEM photomicrograph of monetite (CaHPO_4) powders of WL morphology

Brushite crystallizes in the monoclinic space group Cc with the lattice parameters $a=6.359$, $b=15.177$, $c=5.81$ Å, $\beta=118.54^\circ$ [25]. Triclinic monetite has the following lattice parameters: $a=6.910$, $b=6.627$, $c=6.998$ Å, $\alpha=96.34^\circ$, $\beta=103.82^\circ$, and $\gamma=88.33^\circ$ [25]. The experimentally-determined lattice

parameters of brushite and monetite powders synthesized in this study differed very slightly (only in the third decimal place) from the above-mentioned literature values.

The analysis of FTIR data reproduced in the inset of Fig. 1a revealed the following IR frequencies (in cm^{-1}). The bands at 3544, 3491, 3290, and 3163 were due to the O-H stretching of water. The shoulder at 2955 was again that of O-H stretching. H_2O bending was recorded at 1653 cm^{-1} . The O-H in-plane bending was measured at 1219 cm^{-1} . PO stretching was observed at 1134, 1057, and 987 cm^{-1} . P-O(H) stretching was found at 876 cm^{-1} for the FP (flat-plates) sample, however, its shift to 871 cm^{-1} in the WL (water lily) sample together with the appearance of a carbonate band at 1472 cm^{-1} was indicative of unreacted calcite presence in the WL samples. H_2O libration was observed in both samples at 791 cm^{-1} . Finally, PO bending was recorded at 662, 576, 525 cm^{-1} . The observed IR band positions (of Figs. 1a and 2) were in close agreement with those reported by Xu *et al.* [26].

Both brushite powders were largely transformed into octacalcium phosphate (OCP, $\text{Ca}_8(\text{HPO}_4)_2(\text{PO}_4)_4 \cdot 5\text{H}_2\text{O}$) upon one week of soaking in DMEM solution at 36.5 C , as shown by the X-ray diffraction data of Fig. 3a. WL samples still contained some unreacted brushite phase after 1 week in DMEM, but the FP samples were able to completely transform into OCP. Even after 48 h of ageing (pH dropping from the initial 7.4 to around 6.8) in the non-replenished DMEM solutions, OCP was the major phase in the FP samples. The lattice parameters of the triclinic OCP phase determined from the FP-1 week sample (Fig. 3a, top trace) were $a=9.530$, $b=18.991$, $c=6.854 \text{ \AA}$, $\alpha=92.30^\circ$, $\beta=90.11^\circ$, and $\gamma=79.94^\circ$, and they were in close agreement with those reported in ICDD PDF 026-1056 [27]. The FTIR data of the above samples were depicted in Fig. 3b, which were in good agreement with those previously reported by Wu and Nancollas [28], Suzuki *et al.* [29], LeGeros *et al.* [30], and LeGeros [31].

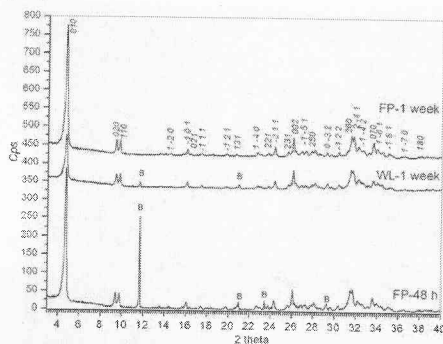


Fig. 3a XRD traces of WL- and FP-type brushite powders soaked in DMEM solution at 36.5 C (times indicated soaking periods); FP-1 week trace showing single-phase OCP together with the crystallographic indices of the OCP phase; letter B indicated the brushite peaks

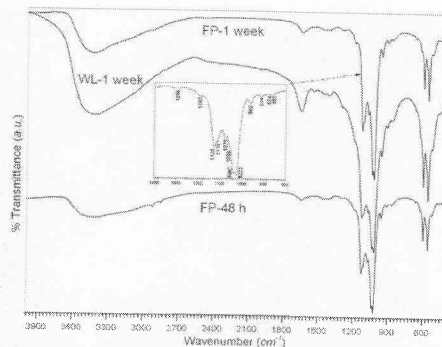


Fig. 3b FTIR traces of WL- and FP-type brushite powders soaked in DMEM solution at 36.5 C ; the inset is showing the detail over the 1400 to 800 cm^{-1} range of the FP-1 week samples

The following IR bands were observed in the FTIR spectrum of FP-1 week sample shown in Fig. 3b. H-O-H or crystalline water of OCP was assigned to the wide band recorded over the range of $3700\text{-}3000 \text{ cm}^{-1}$. H_2O bending was at 1647 cm^{-1} . The P-OH bending modes originating from the HPO_4 groups of OCP were observed at 1296 and 1193 cm^{-1} . P-O in HPO_4 and PO_4 groups were recorded at 1126 , 1110 , 1075 , 1058 , 1040 , 1023 , 962 , 628 , 603 , 560 , 471 , and 452 cm^{-1} . The P-OH stretching

mode of HPO_4 groups was at 914 and 871 cm^{-1} . The IR band assignment was in good agreement with those reported by LeGeros *et al.* [30].

The changes occurred in the particles of brushite at 36.5 C were followed by the SEM photomicrographs. It was found that one week was enough to fully convert brushite to OCP, as supported by the FTIR and XRD data.

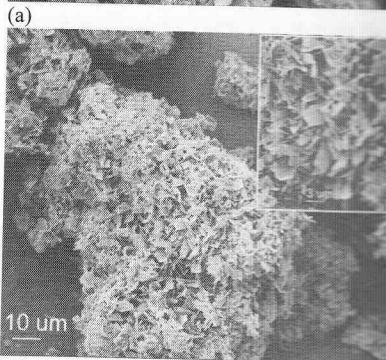


Fig. 4 SEM photomicrographs of brushite particles (a) WL - 24 h, (b) WL - 72 h

The DMEM solution used in this study was prepared by dissolving the brushite powders synthesized in this study. It must be noted that the brushite was dissolved in DMEM solutions at 37 C , under similar conditions, with the brushite powder.

In the current study, the DMEM solution was prepared in clean and sealed glass media bottles at 37 C . This finding indicated that the DMEM solution was in the brushite phase. In stark contrast to this, if one had used a brushite powder contained in a clean, sealed bottle (whether brushite or apatite) produced lots of apatitic CaP precipitates by

mode of HPO_4 groups was at 914 and 874 cm^{-1} . Finally, the HO-PO_3 bending mode in HPO_4 was found at 525 cm^{-1} . The IR band assignments of the FP-1 week samples of this study were in good agreement with those reported by LeGeros *et al.* [30, 31].

The changes occurred in the particle morphology of brushite powders aged in DMEM solutions at 36.5 C were followed by the SEM photomicrographs given in Figures 4a through 4d. It was found that one week was enough to fully convert the brushite crystals into octacalcium phosphate, as also supported by the FTIR and XRD data.

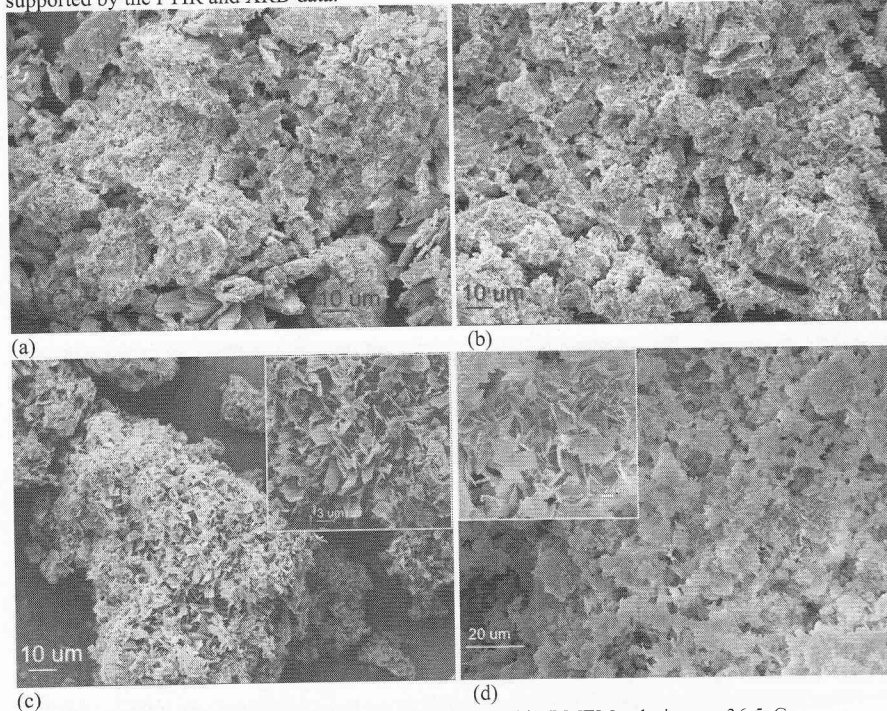


Fig. 4 SEM photomicrographs of samples soaked in DMEM solutions at 36.5 C ; (a) WL - 24 h, (b) WL - 72 h, (c) WL - 1 week, (d) FP - 1 week

The DMEM solution used in this study was shown to be a convenient and robust medium to synthesize OCP powders in a static glass medium bottle, heated at 36.5 C , by starting with brushite powders synthesized in this study. It must be remembered that brushite powders soaked in SBF solutions at 37 C , under similar conditions, were only transforming into apatite [7-21].

In the current study, the DMEM solutions aged alone (i.e., without any brushite powders) in clean and sealed glass media bottles at 37 C for one week did not produce any precipitates within the bottles. This finding indicated that the DMEM solutions were not autogenously precipitating the OCP phase. In stark contrast to this, if one heated a volume of freshly prepared SBF solution, to be contained in a clean, sealed bottle (whether glass or plastic) at 36.5 C for one week, it would have produced lots of apatitic CaP precipitates by itself. How can one use such a medium to test bioactivity?

osteoblasts in culture (such as alkaline phosphatase activity, lactate production, proline hydroxylation, DNA content and thymidine incorporation), interested readers may consult the article by Kaysinger and Ramp [45].

If, for example, a Tris-buffered SBF solution cannot allow its pH to drop from 7.4 to around 6.5-6.9, then it could not be possible for such a solution to mimic any osteoclast resorptive activity. Such a solution seems to be only programmed to heterogeneously nucleate nano-textured HA crystallites on the immersed substrates which do not cause a shift in the solution pH value towards 6.5 to 7. Hydroxylated surfaces ease this HA nucleation, and the pre-soaking of titanium coupons in heated solutions of NaOH or KOH prior to the SBF immersion constitutes a good example.

Calcification in cell culture media is a well-known phenomenon. For example, de Jonge *et al.* [45] very recently reported that soaking titanium and calcium phosphate-coated titanium substrates in α -MEM (supplemented with fetal calf or bovine serum (FBS), ascorbic acid, glycerophosphate and gentamycin) solutions at 37 °C led to the formation of apatitic calcium phosphate calcification on those. However, de Jonge *et al.* [46] did not report the formation of OCP. The presence or absence of FBS in cell culture media exerts a significant difference on the calcification products.

There surely is a difference in the calcification potentials of α -MEM (minimum essentials medium Eagle, α -modification) and DMEM solutions, and this was best explored in the study of Coelho *et al.* [47] performed on the human osteoblastic cell cultures. DMEM is a less nutrient-rich medium with respect to amino acids and vitamins, although, nutrient concentrations are, on the whole, higher than those found in α -MEM [47]. α -MEM contains ascorbic acid, and less NaHCO₃ (27 mM) than that found in DMEM (44 mM). Coelho *et al.* [47] reported the formation of slightly higher amounts of apatitic calcium phosphate spherules (but not OCP) in DMEM solutions after culturing the osteoblasts for more than four weeks, by providing SEM photomicrographs and EDXS analysis results.

Interestingly, Price *et al.* [48] found in their calcification studies on rat aortas soaked in DMEM solutions alone were not able to form any calcification products; however, DMEM solutions supplemented with 1.5% human, bovine or rat blood serum were able to form apatitic calcification products easily on the same rat aortas. Price *et al.* [48] attributed this behaviour to the presence of a potent serum calcification factor (i.e., the noncollagenous serum protein fetuin) in serum.

Therefore, in comparing the Coelho *et al.* [47] and Price *et al.* [48] studies one should realize that in the first study the DMEM solutions contained osteoblasts and the alkaline phosphatase (ALP) released from the osteoblasts would appear in the medium, whereas in the latter study there were no osteoblasts to secrete ALP and hence the serum calcification factors.

Until now, OCP crystallization was more or less considered to take place in aqueous solutions containing monocarboxylates, such as acetate (or formate) ions; this was probably due to the quite influential papers by Newesely [49] and LeGeros [31] on OCP synthesis. These synthesis procedures involved the mixing of calcium nitrate solutions with sodium acetate solutions or calcium acetate solutions with sodium phosphate solutions, respectively. LeGeros procedure envisaged the precipitation process to be performed between 60 and 80 °C [31]. Liu *et al.* [50] slightly modified the Newesely procedure of OCP synthesis, mixed calcium nitrate and disodium hydrogen phosphate solutions in a sodium acetate solution, continued the precipitation-maturation process at 45 °C for 48 h, but were not able to obtain single-phase OCP powders according to their FTIR spectra. Brown *et al.* [32] have historically been the first to hydrolyze brushite powders in a concentrated sodium acetate solution, and the same procedure was recently repeated by Monma *et al.* [51]. Our study, on the other hand, demonstrated a new route which totally eliminated the use of quite concentrated (0.2 M [50] or 0.5 M [51]) acetate solutions for synthesizing the OCP powders.

The absence of any previous studies related to the ageing/immersion of brushite crystals or powders, at the human body temperature of 36.5 °C, in a DMEM solution containing amino acids, the

present authors are somewhat compelled to search for studies performed on titanium by using other calcification solutions.

Wen *et al.* [53] observed the formation of an OCP-like phase on the surface of HCl-H₂SO₄ and NaOH-treated commercially pure titanium immersed into a Tris/HCl-buffered and Mg- and HCO₃⁻-free supersaturated calcification solution, SCS, having a Ca/P molar ratio of 1.67. This solution was, therefore, different from the popular SBF solutions also in terms of its Ca/P molar ratio and its degree of supersaturation with respect to apatite nucleation. The absence of Mg²⁺ and HCO₃⁻ ions in the solution described by Wen *et al.* [52] and the observation of OCP in place of single-phase apatite must be underlined. Wen and Moradian-Oldak [53] later reported the formation of OCP (instead of apatite) on titanium surfaces immersed in Mg- and HCO₃⁻-free and Tris-buffered supersaturated calcification solutions (SCS) both without and with bovine serum albumin or murine amelogenin. These two reports [52, 53], contributed by the same first author, seemed to assert a significant difference in terms of the phase nature of the calcium phosphate deposited by the SCS (Mg- and HCO₃⁻-free) and SBF (Mg- and HCO₃⁻-containing) solutions. The same Mg- and HCO₃⁻-free SCS solution, originally reported in the Wen *et al.* [52] paper, was then reproduced and reported in a number of seemingly follow-up studies to form OCP deposits on titanium [54, 55] or HA or HA-TCP bioceramics [56].

However, the Hepes-buffered DMEM solution used in our study contained both Mg²⁺ and HCO₃⁻ ions, and was still able to completely transform the immersed brushite powders into OCP in 7 days. Therefore, the crystallization of OCP from a Tris-buffered SCS (without Mg and HCO₃⁻) or Hepes-buffered DMEM solution cannot be simply attributed to or explained by the absence or presence of Mg²⁺ and HCO₃⁻ ions. The main question here should again be focused on the pH-stability of solutions buffered by using Tris or Hepes. Wen *et al.* [52] reported that the pH of their SCS solutions started from 7.4 and gradually dropped to around 7.2 within the first 16 h of immersion. This rapid drop in pH should be the reason for forming OCP instead of HA on their titanium coupons.

A possible answer to this issue was provided by an article of Serro and Saramago [57]. Serro and Saramago [57] prepared a new solution designated as SBF0, with the same composition of Kokubo SBF [1] but without the buffer Tris. The buffer TRIS, present in SBF, is known to form soluble complexes with several cations, including the most important Ca²⁺. This would in turn help to reduce the concentration of free Ca²⁺ ions in SBF with respect to an SBF-like solution without Tris [57]. The pH of DMEM solutions (containing the brushite powders) of the current study decreased from 7.4 to around 6.77 by the end of the first 72 hours at 36.5 C, then gradually rose to 6.83 over the following 48 hours of immersion. The pH values of the brushite-containing DMEM solutions were found to rise to 7.0 at the end of 7 days at 36.5 C. This meant that the Hepes-buffered DMEM solutions were not able to maintain the initial pH of 7.4 when they had the slightly acidic brushite powders in them. The SBF-without-Tris solutions of Serro and Saramago [57], on the other hand, aged at 37 C were found to exhibit pH values increasing from 7.4 to values of 8.5 (while precipitating HA) in the course of 7 days, whereas the same authors reported the corresponding pH variations for Tris-buffered SBF solutions to be below 0.1 within the same timeframe. Does this mean that maintaining the pH value at or not below 7.4 would be essential for producing HA from such solutions?

The morphology of the OCP crystals deposited on titanium, HA or HA-TCP samples [52-56] of previous studies were quite similar to those shown in Figs. 4c and 4d.

The influence of amino acids present in MEM solutions, in direct comparison to HBSS (Hanks' balanced salt solution) [58], was studied by Hiromoto *et al.* [59] in terms of the amount of calcium phosphate deposited on titanium coupons immersed in HBSS (Hanks' balanced salt solution) or MEM solutions over 7 days. HBSS solutions do not contain amino acids and any Tris or Hepes buffers [58]. The presence of biomolecules (in the case of MEM solutions) was found to decrease the amount of calcium phosphate deposited [59]. One of the most important contributions of the Hiromoto *et al.* [59] study had been the quantitative measurement of the Ca, P, C, N, and O amounts of the surface oxide

films of titanium specimens immersed in spectroscopy. Quite small amounts of calcium phosphate layers coated on titanium in the MEM solutions. Hiromoto *et al.* [59] studied the incorporation of biomolecules, supplied by calcium phosphate phases in such biocompatible

Although the experimental scope of the influence of biomolecules (and their occurrence) in DMEM at 36.5 C, it shall be noted that our OCP crystals.

The role of bovine serum albumin (BSA) of bovine origin in metastable supersaturated solutions [60]. BSA was found to strongly influence the growth rate (g/L), resulting in smaller crystals with curved surfaces. The SEM photomicrographs shown in Figs. 4c and 4d [60] when they synthesized their samples in the

To summarize, if the pH of a physiological buffered SCS [51] is dropping to around 7.0, it would be prone to nucleate crystals of OCP, instead of HA.

DMEM solution was found to have a pH of 36.5 C within 1 week; OCP is a biological product of HA in enamel and bone formation; therefore, the bioactivity of brushite powders as confirmed commonly used in cell culture [61-63], can be tested in the so-called *in vitro* bioactivity testing of brushite.

In regard to follow-up studies, the temperature, if performed in a cell culture, is a viable option to synthesize OCP-based biomolecules, certain proteins and growth factors.

The current study has also offered a new morphology with an unprecedented morphology, i.e., water lily (WL) (water lily)-type brushite or WL-type brushite powders were produced in simple aqueous solutions without substances or surfactants. For example, the morphology of CTAB, a cationic hydrophobic detergent, by the flower-like morphology (i.e., a morphology of brushite synthesis) could only be regarded as an intermediate. It is surely suspected of containing the residues of CTAB, already known to cause chronic toxicity upon the production does eliminate any toxicity (at ppm levels) to be present in such calcium phosphate solutions.

A new family of calcium phosphate crystals, in stark contrast to more common hydroxyapatite, were claimed to show increased *in vivo* resorption. The transformation behavior of brushite at 36.5 C is under study to increase the level of scientific understanding.

films of titanium specimens immersed in HBSS and MEM solutions by using X-ray photoelectron spectroscopy. Quite small amounts of carbon and nitrogen (and especially nitrogen) detected in the calcium phosphate layers coated on titanium were originating directly from the amino acids present in the MEM solutions. Hiromoto *et al.* [59] study thus provided a strong evidence for the adsorption and incorporation of biomolecules, supplied by the amino acids of MEM solutions, in the newly forming calcium phosphate phases in such biocompatible media.

Although the experimental scope of our study was not wide enough to include the investigation of the influence of biomolecules (and their adsorption) on the brushite-to-OCP transformation occurring in DMEM at 36.5 C, it shall be not so unsafe to assume the adsorption of biomolecules on our OCP crystals.

The role of bovine serum albumin (BSA) on the crystallization of OCP on type I collagen of bovine origin in metastable supersaturated solutions of pH=6.5 at 37 C was studied by Combes *et al.* [60]. BSA was found to strongly influence the shape of the OCP crystals at the quite high level of 40 g/L, resulting in smaller crystals with curved edges [60]. The amino acids present in our DMEM solutions did not exhibit such an effect on the crystal morphology of OCP as seen in Figs. 4c and 4d. The SEM photomicrographs shown in Figs. 4c and 4d resembled to those supplied by Combes *et al.* [60] when they synthesized their samples in the absence of BSA.

To summarize, if the pH of a physiologic medium (either Hepes-buffered DMEM or Tris-buffered SCS [51]) is dropping to around 7.2-6.8 during hydrothermal ageing, then such a solution would be prone to nucleate crystals of OCP, rather than those of HA.

DMEM solution was found to have the ability of transforming brushite powders into OCP at 36.5 C within 1 week; OCP is a biological calcium phosphate phase; OCP is indeed the precursor to HA in enamel and bone formation; therefore, the DMEM solutions can be used to test the so-called bioactivity of brushite powders as confidently as SBF solutions. DMEM solutions, which are commonly used in cell culture [61-63], can be regarded as a feasible alternative to using SBF solutions in the so-called *in vitro* bioactivity testing of synthetic biomaterials.

In regard to follow-up studies, the transformation of brushite powders to OCP at the human body temperature, if performed in a cell culture solution such as DMEM, could also prove to be a viable option to synthesize OCP-based biomaterials in solutions, which can be specifically loaded with bioactive molecules, certain proteins and growth factors.

The current study has also offered a new synthesis route to prepare $\text{CaHPO}_4 \cdot 2\text{H}_2\text{O}$ powders with an unprecedented morphology, i.e., water lily(WL)-like brushite dumbbells. The main advantage of the WL (water lily)-type brushite or WL-type monetite powders will be the following. These powders were produced in simple aqueous systems which did not contain any organic or polymeric substances or surfactants. For example, the very recent use of cetyltrimethylammonium bromide (CTAB, a cationic hydrophobic detergent), by Ruan *et al.* [64], in preparing monetite powders with a flower-like morphology (i.e., a morphology outside the common flat plate-type observed in brushite synthesis) could only be regarded as an interesting attempt, but the resultant monetite powders must surely be suspected of containing the residues of CTAB used during synthesis. CTAB, for instance, is already known to cause chronic toxicity upon its digestion [65, 66]. The total absence of organics in the production does eliminate any toxicity concerns about the possible organic residues (even at the ppm levels) to be present in such calcium phosphate-based bone substitute biomaterials.

A new family of calcium phosphate cements with the final setting product being brushite (in stark contrast to more common hydroxyapatite cements) was developed within the last decade and they were claimed to show increased *in vivo* resorbability [67-69]. The investigation of the hydrothermal transformation behavior of brushite at 36.5 C in a cell culture medium, such as DMEM, was expected to increase the level of scientific understanding on the bioactivity of brushite-based biomaterials.

CONCLUSIONS

- (1) A new chemical process was suggested for the robust and economical synthesis of brushite ($\text{CaHPO}_4 \cdot 2\text{H}_2\text{O}$) powders with a unique water lily-like morphology. The new process involved the simple stirring of an aqueous suspension of precipitated calcite (CaCO_3) powders and dissolved ammonium dihydrogen phosphate ($\text{NH}_4\text{H}_2\text{PO}_4$), the suspension being free of any organic additives, at room temperature ($24 \pm 1^\circ\text{C}$), from 6 to 60 minutes.
- (2) The results showed that it was possible to preserve the water lily-like particle morphology of brushite even though the powders were later converted to monetite (CaHPO_4) by heating at 200°C . Monetite powders with water lily-shaped crystals were produced for the first time.
- (3) This study offered a simple procedure for producing octacalcium phosphate ($\text{Ca}_8(\text{HPO}_4)_2(\text{PO}_4)_4 \cdot 5\text{H}_2\text{O}$) powders, upon straightforward immersion of brushite powders in DMEM solutions (pH 7.4) at the human body temperature of 36.5°C . The highest temperature of processing hereby used in the manufacture of bulk, well-crystallized OCP powders was 36.5°C .

Notes: Certain commercial equipment, instruments, solutions or chemicals are only identified in this paper to foster understanding. Such identification does not imply recommendation or endorsement by the authors, nor does it imply that the equipment or materials identified are necessarily the best available for the purpose.

REFERENCES

- [1] T. Kokubo, Surface Chemistry of Bioactive Glasses, *J. Non-Cryst. Solids*, **120**, 138-151 (1990).
- [2] D. Bayraktar and A.C. Tas, Chemical Preparation of Carbonated Calcium Hydroxyapatite Powders at 37°C in Urea-containing Synthetic Body Fluids, *J. Eur. Ceram. Soc.*, **19**, 2573-2579 (1999).
- [3] H.M. Kim, K. Kishimoto, F. Miyaji, T. Kokubo, T. Yao, Y. Suetsugu, J. Tanaka, and T. Nakamura, Composition and Structure of Apatite Formed on Organic Polymer in Simulated Body Fluid with a High Content of Carbonate Ion, *J. Mater. Sci. Mater. M.*, **11**, 421-426 (2000).
- [4] M. Bohner and J. Lemaitre, Can Bioactivity be Tested in vitro with SBF Solution? *Biomaterials*, **30**, 2175-2179 (2009).
- [5] T. Kokubo and H. Takadama, How Useful Is SBF in Predicting in vivo Bone Bioactivity? *Biomaterials*, **27**, 2907-2915 (2006).
- [6] F.C.M. Driessens and R.M.H. Verbeeck, *Biomaterials*, pp. 37-59, CRC Press, Boca Raton, FL, 1990.
- [7] M. Kumar, H. Dasarathy, and C. Riley, Electrodeposition of Brushite Coatings and Their Transformation to Hydroxyapatite in Aqueous Solutions, *J. Biomed. Mater. Res.*, **45**, 302-310 (1999).
- [8] D. Walsh and J. Tanaka, Preparation of Bone-like Apatite Foam Cement, *J. Mater. Sci. Mater. M.*, **12**, 339-343 (2001).
- [9] L. Grondahl, F. Cardona, K. Chiem, E. Wentrup-Byrne, and T. Bostrom, Calcium Phosphate Nucleation on Surface-modified PTFE Membranes, *J. Mater. Sci. Mater. M.*, **14**, 503-510 (2003).
- [10] S.J. Lin, R.Z. LeGeros, and J.P. LeGeros, Adherent Octacalcium Phosphate Coating on Titanium Alloy using Modulated Electrochemical Deposition Method, *J. Biomed. Mater. Res.*, **66A**, 819-828 (2003).
- [11] C.Y. Kim and H.B. Lim, Hardening and Hydroxyapatite Formation on Bioactive Glass and Glass-ceramic Cement, *Key Eng. Mater.*, **254-2**, 305-308 (2004).
- [12] H.S. Azevedo, I.B. Leonor, C.M. Alves, and R.L. Reis, Incorporation of Proteins and Enzymes at Different Stages of the Preparation of Calcium Phosphate Coatings on a Degradable Substrate by a Biomimetic Methodology, *Mater. Sci. Eng. C*, **25**, 169-179 (2005).
- [13] X. Lu and Y. Leng, Theoretical Analysis of Calcium Phosphate Precipitation in Simulated Body Fluid, *Biomaterials*, **26**, 1097-1108 (2005).
- [14] D.J.T. Hill-Zainuddin, T.V. Chirila, A. HEMA-based Hydrogels in the Presence of *Biomacromolecules*, **7**, 1758-1765 (2006).
- [15] J. Pena, I. Barba-Izquierdo, A. M. Chitosan/Apatite Materials at Room Temper
- [16] T. Anada, T. Kumagai, Y. Honda, T. dependent Osteogenic Effect of Octacalcium *Eng.*, **14**, 965-978 (2008).
- [17] C. Knabe, A. Houshmand, G. Berger, P. of Rapidly Resorbable Bone Substitute M. *Phenotype in vitro, J. Biomed. Mater. Res.*
- [18] F. Yang, J.G.C. Wolke, and J.A. Jansen, Poly(epsilon-caprolactone) Scaffolds for B (2008).
- [19] J.A. Juhasz, S.M. Best, A.D. Auffret, a Simulated Body Fluid and Human Blood Ser
- [20] L.P. Xu, E.L. Zhang, and K. Yang, Ph Zn Alloy for Biomedical Application, *J. Man*
- [21] A. Rakngarm and Y. Mutoh, Electrodepos Titanium and Ti-6Al-4V in Two Types of E 275-283 (2009).
- [22] S. Mandel and A.C. Tas, Br ($\text{Ca}_8(\text{HPO}_4)_2(\text{PO}_4)_4 \cdot 5\text{H}_2\text{O}$) Transformation in 254 (2010).
- [23] A.C. Tas, Porous, Biphasic CaCO_3 -C Calcite (CaCO_3) Powder, *Int. J. Appl. Ceram.*
- [24] S. Jalota, S.B. Bhaduri, and A.C. Tas, HCO_3^- to Make Bone Substitutes More Osteo
- [25] L. Tortet, J.R. Gavarrri, G. Nihoul, and A. (brushite) and CaHPO_4 (monetite) by Infran *Chem.*, **132**, 6-16 (1997).
- [26] J. Xu, I.S. Butler, and D.F.R. Gilson, Studies of Dicalcium Phosphate Dihydrate (CaHPO_4), *Spectrochimica Acta A*, **55**, 2801-2
- [27] ICDD PDF: International Centre for Diff
- [28] W. Wu and G.H. Nancollas, Nucleati Titanium Oxide Surfaces, *Langmuir*, **13**, 861-4
- [29] O. Suzuki, S. Kamakura, T. Katagiri, M. Formation Enhanced by Implanted Octacalcium Hydroxyapatite, *Biomaterials*, **27**, 2671-2681
- [30] R.Z. LeGeros, G. Daculsi, I. Orly, T. Ab of Octacalcium Phosphate (OCP) to Apatite, *S*
- [31] R.Z. LeGeros, Preparation of Octacalcium *Tissue Int.*, **37**, 194-197 (1985).
- [32] W.E. Brown, J.P. Smith, J.R. Lehr, and between Octacalcium Phosphate and Hydroxy
- [33] E.C. Moreno, T.M. Gregory and W.E. Br Pairs in System $\text{Ca}(\text{OH})_2$ - H_3PO_4 - H_2O at 37.5°C

- [14] D.J.T. Hill-Zainuddin, T.V. Chirila, A.K. Whittaker, and A. Kemp, Experimental Calcification of HEMA-based Hydrogels in the Presence of Albumin and a Comparison to the in vivo Calcification, *Biomacromolecules*, **7**, 1758-1765 (2006).
- [15] J. Pena, I. Barba-Izquierdo, A. Martinez, and M. Vallet-Regi, New Method to Obtain Chitosan/Apatite Materials at Room Temperature, *Solid State Sciences*, **8**, 513-519 (2006).
- [16] T. Anada, T. Kumagai, Y. Honda, T. Masuda, R. Kamijo, S. Kamakura, and O. Suzuki, Dose-dependent Osteogenic Effect of Octacalcium Phosphate on Mouse Bone Marrow Stromal Cells, *Tissue Eng.*, **14**, 965-978 (2008).
- [17] C. Knabe, A. Houshmand, G. Berger, P. Ducheyne, R. Gildenharr, I. Kranz, and M. Stiller, Effect of Rapidly Resorbable Bone Substitute Materials on the Temporal Expression of the Osteoblastic Phenotype in vitro, *J. Biomed. Mater. Res.*, **84A**, 856-868 (2008).
- [18] F. Yang, J.G.C. Wolke, and J.A. Jansen, Biomimetic Calcium Phosphate Coating on Electrospun Poly(epsilon-caprolactone) Scaffolds for Bone Tissue Engineering, *Chem. Eng. J.*, **137**, 154-161 (2008).
- [19] J.A. Juhasz, S.M. Best, A.D. Auffret, and W. Bonfield, Biological Control of Apatite Growth in Simulated Body Fluid and Human Blood Serum, *J. Mater. Sci. Mater. M.*, **19**, 1823-1829 (2008).
- [20] L.P. Xu, E.L. Zhang, and K. Yang, Phosphating Treatment and Corrosion Properties of Mg-Mn-Zn Alloy for Biomedical Application, *J. Mater. Sci. Mater. M.*, **20**, 859-867 (2009).
- [21] A. Rakngarm and Y. Mutoh, Electrodeposition of Calcium Phosphate Film on Commercial Pure Titanium and Ti-6Al-4V in Two Types of Electrolyte at Room Temperature, *Mater. Sci. Eng. C*, **29**, 275-283 (2009).
- [22] S. Mandel and A.C. Tas, Brushite ($\text{CaHPO}_4 \cdot 2\text{H}_2\text{O}$) to Octacalcium Phosphate ($\text{Ca}_8(\text{HPO}_4)_2(\text{PO}_4)_4 \cdot 5\text{H}_2\text{O}$) Transformation in DMEM Solutions at 36.5 C, *Mater. Sci. Eng. C*, **30**, 245-254 (2010).
- [23] A.C. Tas, Porous, Biphasic CaCO_3 -Calcium Phosphate Biomedical Cement Scaffolds from Calcite (CaCO_3) Powder, *Int. J. Appl. Ceram. Technol.*, **4**, 152-163 (2007).
- [24] S. Jalota, S.B. Bhaduri, and A.C. Tas, Using a Synthetic Body Fluid (SBF) Solution of 27 mM HCO_3^- to Make Bone Substitutes More Osteointegrative, *Mater. Sci. Eng. C*, **28**, 129-140 (2008).
- [25] L. Tortet, J.R. Gavarri, G. Nihoul, and A.J. Dianoux, Study of Protonic Mobility in $\text{CaHPO}_4 \cdot 2\text{H}_2\text{O}$ (brushite) and CaHPO_4 (monetite) by Infrared Spectroscopy and Neutron Scattering, *J. Solid State Chem.*, **132**, 6-16 (1997).
- [26] J. Xu, I.S. Butler, and D.F.R. Gilson, FT-Raman and High-Pressure Infrared Spectroscopic Studies of Dicalcium Phosphate Dihydrate ($\text{CaHPO}_4 \cdot 2\text{H}_2\text{O}$) and Anhydrous Calcium Phosphate (CaHPO_4), *Spectrochimica Acta A*, **55**, 2801-2809 (1999).
- [27] ICDD PDF: International Centre for Diffraction Data, Powder Diffraction File. PA, USA.
- [28] W. Wu and G.H. Nancollas, Nucleation and Crystal Growth of Octacalcium Phosphate on Titanium Oxide Surfaces, *Langmuir*, **13**, 861-865 (1997).
- [29] O. Suzuki, S. Kamakura, T. Katagiri, M. Nakamura, B. Zhao, Y. Honda, and R. Kamijo, Bone Formation Enhanced by Implanted Octacalcium Phosphate involving Conversion into Ca-deficient Hydroxyapatite, *Biomaterials*, **27**, 2671-2681 (2006).
- [30] R.Z. LeGeros, G. Daculsi, I. Orly, T. Abergas, and W. Torres, Solution-mediated Transformation of Octacalcium Phosphate (OCP) to Apatite, *Scanning Microscopy*, **3**, 129-138 (1989).
- [31] R.Z. LeGeros, Preparation of Octacalcium Phosphate (OCP): A Direct Fast Method, *Calcified Tissue Int.*, **37**, 194-197 (1985).
- [32] W.E. Brown, J.P. Smith, J.R. Lehr, and A.W. Frazier, Crystallographic and Chemical Relations between Octacalcium Phosphate and Hydroxyapatite, *Nature*, **196**, 1048-1050 (1962).
- [33] E.C. Moreno, T.M. Gregory and W.E. Brown, Solubility of $\text{CaHPO}_4 \cdot 2\text{H}_2\text{O}$ and Formation of Ion Pairs in System $\text{Ca}(\text{OH})_2\text{-H}_3\text{PO}_4\text{-H}_2\text{O}$ at 37.5 C, *J. Res. Natl. Bur. Std.*, **70A**, 545-552 (1966).

- [34] M. Iijima, Formation of Octacalcium Phosphate in vitro, *Monogr. Oral Sci.*, **18**, 17-49 (2001).
- [35] L.J. Shyu, L. Perez, S.L. Zawacki, J.C. Heughebaert, and G.H. Nancollas, The Solubility of Octacalcium Phosphate at 37 °C in the System $\text{Ca}(\text{OH})_2\text{-H}_3\text{PO}_4\text{-KNO}_3\text{-H}_2\text{O}$, *J. Dent. Res.*, **62**, 398-400 (1983).
- [36] X. Guan, R. Tang and G.H. Nancollas, The Potential Calcification of Octacalcium Phosphate on Intraocular Lens Surfaces, *J. Biomed. Mater. Res.*, **71A**, 488-496 (2004).
- [37] H.E.L. Madsen, The Growth of Dicalcium Phosphate Dihydrate on Octacalcium Phosphate at 25 °C, *J. Cryst. Growth*, **80**, 450-452 (1987).
- [38] H.E.L. Madsen, Influence of Foreign Metal Ions on Crystal Growth and Morphology of Brushite ($\text{CaHPO}_4 \cdot 2\text{H}_2\text{O}$) and its Transformation to Octacalcium Phosphate and Apatite, *J. Cryst. Growth*, **310**, 2602-2612 (2008).
- [39] R.Z. Sabirov, J. Prenen, G. Droogmans, and B. Nilius, Extra- and Intracellular Proton-binding Sites of Volume-regulated Anion Channels, *J. Membrane Biol.*, **177**, 13-22 (2000).
- [40] L. Fulop, G. Szigeti, J. Magyar, N. Szentandrassy, T. Ivanics, Z. Miklos, L. Ligeti, A. Kovacs, G. Szenasi, L. Csernoch, P.P. Nanasi, and T. Banyasz, Differences in Electrophysiological and Contractile Properties of Mammalian Cardiac Tissues Bathed in Bicarbonate- and HEPES-buffered Solutions, *Acta Physiol. Scand.*, **178**, 11-18 (2003).
- [41] J. Pratt, J.D. Cooley, C.W. Purdy, and D.C. Straus, Lipase Activity from Strains of *Pasteurella Multocida*, *Curr. Microbiol.*, **40**, 306-309 (2000).
- [42] T. Nordstrom, L.D. Shrode, O.D. Rotstein, R. Romanek, T. Goto, J.N.M. Heersche, M.F. Manolson, G.F. Brisseau, and S. Grinstein, Chronic Extracellular Acidosis Induces Plasmalemmal Vacuolar type H^+ ATPase Activity in Osteoclasts, *J. Biol. Chem.*, **272**, 6354-6360 (1997).
- [43] A.F. Schilling, W. Linhart, S. Filke, M. Gebauer, T. Schinke, J.M. Rueger, and M. Amling, Resorbability of Bone Substitute Biomaterials by Human Osteoclasts, *Biomaterials*, **25**, 3963-3972 (2004).
- [44] A. Brandao-Burch, J.C. Utting, I.R. Orriss, and T.R. Arnett, Acidosis Inhibits Bone Formation by Osteoblasts in vitro by Preventing Mineralization, *Calcified Tissue Int.*, **77**, 167-174 (2005).
- [45] K.K. Kaysinger and W.K. Ramp, Extracellular pH Modulates the Activity of Cultured Human Osteoblasts, *J. Cell. Biochem.*, **68**, 83-89 (1998).
- [46] L.T. de Jonge, J.J.J.P. van den Beucken, S.C.G. Leeuwenburgh, A.A.J. Hamers, J.G.C. Wolke, and J.A. Jansen, The Osteogenic Effect of Electrospayed Nanoscale Collagen/Calcium Phosphate Coatings on Titanium, *Biomaterials*, **31**, 2461-2469 (2010).
- [47] M.J. Coelho, A.T. Cabral, and M.H. Fernandes, Human Bone Cell Cultures in Biocompatibility Testing. Part I: Osteoblastic Differentiation of Serially Passaged Human Bone Marrow Cells Cultured in α -MEM and in DMEM, *Biomaterials*, **21**, 1087-1094 (2000).
- [48] P.A. Price, W.S. Chan, D.M. Jolson, and M.K. Williamson, The Elastic Lamellae of Devitalized Arteries Calcify when Incubated in Serum – Evidence for a Serum Calcification Factor, *Arterioscl. Throm. Vas.*, **26**, 1079-1085 (2006).
- [49] E. Hayek and H. Newesely, Pentacalcium Monohydroxyorthophosphate, *Inorg. Syn.*, **7**, 63-65 (1963).
- [50] Y. Liu, P.R. Cooper, J.E. Barralet, and R.M. Shelton, Influence of Calcium Phosphate Crystal Assemblies on the Proliferation and Osteogenic Gene Expression of Rat Bone Marrow Stromal Cells, *Biomaterials*, **28**, 1393-1403 (2007).
- [51] H. Monma and T. Kamiya, Preparation of Hydroxyapatite by the Hydrolysis of Brushite, *J. Mater. Sci.*, **22**, 4247-4250 (1987).
- [52] H.B. Wen, J.G.C. Wolke, J.R. de Wijn, Q. Liu, F.Z. Cui, and K. de Groot, Fast Precipitation of Calcium Phosphate Layers on Titanium Induced by Simple Chemical Treatments, *Biomaterials*, **18**, 1471-1478 (1997).
- [53] H.B. Wen and J. Moradian-Oldak, Recombinant Amelogenin, *J. Biomed. Mater. Res.*, **66A**, 779-788 (2004).
- [54] F. Barrere, P. Layrolle, C.A. van Blitterswijk, A Crystal Growth Study of Octacalcium Phosphate, *J. Biomed. Mater. Res.*, **66A**, 779-788 (2004).
- [55] F. Barrere, C.M. van der Valk, R.A. de Groot, and P. Layrolle, Osteogenicity of Octacalcium Phosphate Coating on Osteoblasts, *J. Biomed. Mater. Res.*, **66A**, 779-788 (2004).
- [56] P. Habibovic, C.M. van der Valk, C. Verbeeck, and P. Layrolle, Osteogenicity of Octacalcium Phosphate Coating on Osteoblasts, *J. Biomed. Mater. Res.*, **66A**, 779-788 (2004).
- [57] A.P. Serro and B. Saramago, Influence of Octacalcium Phosphate on Osteoblasts Induced by Incubation in Various Biological Media, *J. Biomed. Mater. Res.*, **66A**, 779-788 (2004).
- [58] J.H. Hanks and R.E. Wallace, Release of Octacalcium Phosphate from a Biomaterial by Refrigeration, *Proc. Soc. Exp. Biol. Med.*, **178**, 11-18 (2003).
- [59] S. Hiromoto, T. Hanawa, and K. Aizawa, Culturing Murine Fibroblasts L929, *Biomaterials*, **25**, 3963-3972 (2004).
- [60] C. Combes, C. Rey, and M. Frechet, Collagen: Influence of Serum Albumin, *J. Biomed. Mater. Res.*, **66A**, 779-788 (2004).
- [61] J.L. Ong, D.R. Villarreal, R. Cavin, and J. J. Webster, Octacalcium Phosphate Coating on Treated Sputtered CaP Surfaces, *J. Mater. Res.*, **15**, 373-380 (2004).
- [62] J.E. Gough, I. Notingher, and L.L. Hench, Octacalcium Phosphate Coating on Titanium: Formation on Rough and Smooth 455S B, *J. Mater. Res.*, **15**, 373-380 (2004).
- [63] T.J. Webster and J.U. Ejirofor, Increased Osteogenicity of Octacalcium Phosphate and CoCrMo, *Biomaterials*, **25**, 4731-4739 (2004).
- [64] Q.C. Ruan, Y.C. Zhu, Y. Zeng, H.L. Zhang, and J. J. Webster, Octacalcium Phosphate Coating on Titanium: Ultrasonic-irradiation-assisted Oriented A, *Chem. B.*, **113**, 1100-1106 (2009).
- [65] B. Isomaa, J. Reuter, and J. J. Webster, Octacalcium Phosphate Coating on Titanium: Cetyltrimethylammonium Bromide (CTAB), *J. Mater. Res.*, **15**, 373-380 (2004).
- [66] M.J. Heffernan, S.P. Kasturi, S.C. Manjunath, and J. J. Webster, Octacalcium Phosphate Coating on Titanium: CD8(+) T Cells by Dendritic Cells Pulsed with Octacalcium Phosphate, *J. Mater. Res.*, **15**, 373-380 (2004).
- [67] B. Flautre, C. Maynou, J. Lemaire, and J. J. Webster, Octacalcium Phosphate Coating on Titanium: TCP Granules Incorporated in Brushite Coating, *J. Mater. Res.*, **15**, 373-380 (2004).
- [68] M. Bohner, F. Theiss, D. Apelt, W. F. M. van der Valk, and B. von Rechenberg, Compositional Control of Octacalcium Phosphate Coating on Titanium: Implantation in Sheep, *Biomaterials*, **24**, 3-10 (2003).
- [69] M. Bohner, U. Gbureck, and J.E. Barralet, Efficient Calcium Phosphate Bone Cement, *J. Mater. Res.*, **15**, 373-380 (2004).

- [53] H.B. Wen and J. Moradian-Oldak, Modification of Calcium Phosphate Coatings on Titanium by Recombinant Amelogenin, *J. Biomed. Mater. Res.*, **64A**, 483-490 (2003).
- [54] F. Barrere, P. Layrolle, C.A. van Blitterswijk, and K. de Groot, Biomimetic Coatings on Titanium: A Crystal Growth Study of Octacalcium Phosphate, *J. Mater. Sci. Mater. M.*, **12**, 529-534 (2001).
- [55] F. Barrere, C.M. van der Valk, R.A.J. Dalmeijer, G. Meijer, C.A. van Blitterswijk, K. de Groot, and P. Layrolle, Osteogenicity of Octacalcium Phosphate Coatings Applied on Porous Metal Implants, *J. Biomed. Mater. Res.*, **66A**, 779-788 (2003).
- [56] P. Habibovic, C.M. van der Valk, C.A. van Blitterswijk, G. Meijer, and K. de Groot, Influence of Octacalcium Phosphate Coating on Osteoinductive Properties of Biomaterials, *J. Mater. Sci. Mater. M.*, **15**, 373-380 (2004).
- [57] A.P. Serro and B. Saramago, Influence of Sterilization on the Mineralization of Titanium Implants Induced by Incubation in Various Biological Model Fluids, *Biomaterials*, **24**, 4749-4760 (2003).
- [58] J.H. Hanks and R.E. Wallace, Relation of Oxygen and Temperature in the Preservation of Tissues by Refrigeration, *Proc. Soc. Exp. Biol. Med.*, **71**, 196-199 (1949).
- [59] S. Hiromoto, T. Hanawa, and K. Asami, Composition of Surface Oxide Film of Titanium with Culturing Murine Fibroblasts L929, *Biomaterials*, **25**, 979-986 (2004).
- [60] C. Combes, C. Rey, and M. Freche, In vitro Crystallization of Octacalcium Phosphate on Type I Collagen: Influence of Serum Albumin, *J. Mater. Sci. Mater. M.*, **10**, 153-160 (1999).
- [61] J.L. Ong, D.R. Villarreal, R. Cavin, and K. Ma, Osteoblast Responses to As-deposited and Heat-treated Sputtered CaP Surfaces, *J. Mater. Sci. Mater. M.*, **12**, 491-495 (2001).
- [62] J.E. Gough, I. Notingher, and L.L. Hench, Osteoblast Attachment and Mineralized Nodule Formation on Rough and Smooth 45S5 Bioactive Glass Monoliths, *J. Biomed. Mater. Res.*, **68A**, 640-650 (2004).
- [63] T.J. Webster and J.U. Ejiogor, Increased Osteoblast Adhesion on Nanophase Metals: Ti, Ti6Al4V, and CoCrMo, *Biomaterials*, **25**, 4731-4739 (2004).
- [64] Q.C. Ruan, Y.C. Zhu, Y. Zeng, H.F. Qian, J.W. Xiao, F.F. Xu, L.L. Zhang, and D.H. Zhao, Ultrasonic-irradiation-assisted Oriented Assembly of Ordered Monetite Nanosheets Stacking, *J. Phys. Chem. B*, **113**, 1100-1106 (2009).
- [65] B. Isomaa, J. Reuter, and B.M. Djupsund, Subacute and Chronic Toxicity of Cetyltrimethylammonium Bromide (CTAB), A Cationic Surfactant, in Rat, *Arch. Toxicol.*, **35**, 91-96 (1976).
- [66] M.J. Heffernan, S.P. Kasturi, S.C. Yang, B. Pulendran, and N. Murthy, The Stimulation of CD8(+) T Cells by Dendritic Cells Pulsed with Polyketal Microparticles Containing Ion-paired Protein Antigen and Poly(inosinic acid)-Poly(cytidylic acid), *Biomaterials*, **30**, 910-918 (2009).
- [67] B. Flautre, C. Maynou, J. Lemaitre, P. Van Landuyt, and P. Hardouin, Bone Colonization of -TCP Granules Incorporated in Brushite Cements, *J. Biomed. Mater. Res.*, **63B**, 413-417 (2002).
- [68] M. Bohner, F. Theiss, D. Apelt, W. Hirsiger, R. Houriet, G. Rizzoli, E. Gnos, C. Frei, J.A. Auer, and B. von Rechenberg, Compositional Changes of a Dicalcium Phosphate Dihydrate Cement after Implantation in Sheep, *Biomaterials*, **24**, 3463-3474 (2003).
- [69] M. Bohner, U. Gbureck, and J.E. Barralet, Technological Issues for the Development of More Efficient Calcium Phosphate Bone Cements: A Critical Assessment, *Biomaterials*, **26**, 6423-6429 (2005).

Advances in Bioceramics and Porous Ceramics IV

Ceramic Engineering and Science Proceedings
Volume 32, Issue 6, 2011

Edited by

Roger Narayan

Paolo Colombo

Volume Editors

Sujanto Widjaja

Dileep Singh

 **WILEY**

The
American
Ceramic
Society





The
American
Ceramic
Society

 **WILEY**
wiley.com

ISBN 978-1-118-05991-3



90000

9 781118 059913

Copyright © 2011 by The American Ceramic Society. All rights reserved.

Published by John Wiley & Sons, Inc., Hoboken, New Jersey.
Published simultaneously in Canada.

No part of this publication may be reproduced, stored in a retrieval system, or transmitted in any form or by any means, electronic, mechanical, photocopying, recording, scanning, or otherwise, except as permitted under Section 107 or 108 of the 1976 United States Copyright Act, without either the prior written permission of the Publisher, or authorization through payment of the appropriate per-copy fee to the Copyright Clearance Center, Inc., 222 Rosewood Drive, Danvers, MA 01923, (978) 750-8400, fax (978) 750-4470, or on the web at www.copyright.com. Requests to the Publisher for permission should be addressed to the Permissions Department, John Wiley & Sons, Inc., 111 River Street, Hoboken, NJ 07030, (201) 748-6011, fax (201) 748-6008, or online at <http://www.wiley.com/go/permission>.

Limit of Liability/Disclaimer of Warranty: While the publisher and author have used their best efforts in preparing this book, they make no representations or warranties with respect to the accuracy or completeness of the contents of this book and specifically disclaim any implied warranties of merchantability or fitness for a particular purpose. No warranty may be created or extended by sales representatives or written sales materials. The advice and strategies contained herein may not be suitable for your situation. You should consult with a professional where appropriate. Neither the publisher nor author shall be liable for any loss of profit or any other commercial damages, including but not limited to special, incidental, consequential, or other damages.

For general information on our other products and services or for technical support, please contact our Customer Care Department within the United States at (800) 762-2974, outside the United States at (317) 572-3993 or fax (317) 572-4002.

Wiley also publishes its books in a variety of electronic formats. Some content that appears in print may not be available in electronic formats. For more information about Wiley products, visit our web site at www.wiley.com.

Library of Congress Cataloging-in-Publication Data is available.

ISBN 978-1-118-05991-3

eBook ISBN: 978-1-118-09526-3
ePDF ISBN: 978-1-118-17264-3

ISSN: 0196-6219

Printed in the United States of America.

10 9 8 7 6 5 4 3 2 1

Preface

Introduction

BIOCERAMICS

Fabrication of Hydroxyapatite

E. K. Girija, G. Suresh Kumar
and S. Narayana Kalkura

Preparation and Protein Adsorption of
Particles for Blood Purification

Jie Li, Yuki Shirotsuki, Satoshi

Collagen-Templated Sol-Gel
Nanotube Mats and Osteoblasts

Song Chen, Toshiyuki Ikoma,
Masaki Takeguchi, and Nobuo

Tissue Ingrowth in Resorbable

Janet Krevolin, James J. Liu,
Hu-Ping Hsu, Cathal Kearney

Selective Laser Sintered Calcium
with Sustained Release of

Bin Duan, William W. Lu, and

Microbeam X-Ray Grain Analysis

Hrishikesh A. Bale, Nobumichi